

RESEARCH

Open Access



Escherichia coli combination with PD-1 blockade synergistically enhances immunotherapy in glioblastoma multiforme by regulating the immune cells

Guochen Li^{1†}, Haiyan Yang^{2†}, Tengfei Ke³, Na Tan¹, Xiaolan Du¹, Xirui Duan¹, Xinyan Zhou¹, Guangrong Zheng^{1*†} and Chengde Liao^{1*†}

Abstract

Background Glioblastoma multiforme (GBM) is the most common and aggressive primary intracranial malignancy. It is characterized by insufficient infiltration of anti-tumor T lymphocytes within the tumor microenvironment (TME), rendering it an “immune cold” disease. This immune deficiency results in poor responses to immune checkpoint blockade (ICB) therapies. Recent studies have demonstrated that bacteria can proliferate within tumors and activate immune responses. Therefore, in this study, we employed *Escherichia coli* (*E. coli*) in combination with anti-PD-1 antibodies to treat GBM, with the aim of exploring the immune-activating potential of *E. coli* in GBM and its synergistic effect on anti-PD-1 therapy.

Methods The *E. coli* and anti-PD-1 antibody therapy were administered intravenously and intraperitoneally, respectively. Complete blood cell count, blood biochemical analysis, hematoxylin and eosin (H&E) staining, and agar plate culture were employed to evaluate the biosafety and tumor-targeting capability of *E. coli*. ELISA kits were used to detect innate immune cytokines. Flow cytometry and immunofluorescence staining were used to investigate T cells. Tumor volume of tumor-bearing mice was recorded to evaluate the combined treatment efficacy. H&E staining and immunofluorescence staining were used to observe the tumor inhibition markers.

Results *E. coli* can specifically target into the tumor region, and activate the innate immune response in mice. Immunofluorescence staining and flow cytometry results demonstrated that the combination treatment group exhibited a significant upregulation of cytotoxic CD8⁺ T cells and a marked suppression of regulatory T cells compared to the control group. The expression of Ki67 was significantly downregulated, and TUNEL staining revealed an increased number of apoptotic cells in the combination treatment group. Furthermore, the tumor growth rate in the combination treatment group was significantly slower than that in the control group.

[†]Guochen Li and Haiyan Yang have contributed equally to this work.

[†]Guangrong Zheng and Chengde Liao are corresponding authors.

*Correspondence:

Guangrong Zheng
zhengguangrong@kmmu.edu.cn
Chengde Liao
chengdeliao@qq.com

Full list of author information is available at the end of the article



Conclusions *E. coli* exhibits potential anti-tumor activity and can activate the innate immune response and further regulate immune cells in the tumor tissues to synergize the effect of anti-PD-1 therapy on GBM, providing new insights to enhance the efficacy of GBM immunotherapy.

Keywords Glioblastoma, PD-1, *Escherichia coli*, Immunotherapy, Synergy

Background

Glioblastoma multiforme (GBM) presents the most common and aggressive primary intracranial malignancy, with a poor prognosis and a median survival of only 14.6 months after diagnosis [1]. Surgical resection, radiotherapy, and chemotherapy are standard treatments, but limited by the proliferative nature and the blood–brain barrier (BBB) [2–4]. In recent years, immunotherapy has been extensively studied in the treatment of GBM [5], but the lack of anti-tumor immune cells within the tumor greatly reduces the efficacy of immunotherapy [6, 7]. Therefore, it is urgent to increase the infiltration of immune cells within the tumor in response to the reactivation of T cells caused by immunotherapy.

Among immune checkpoint targets, monoclonal antibodies directed against programmed cell death protein-1 (PD-1) or programmed cell death-ligand 1 (PD-L1) were globally employed for immunotherapy in many cancers such as non-small cell lung cancer (NSCLC), hepatocellular carcinoma, and melanoma [8]. However, GBM is commonly regarded as an “immunologically cold” tumor [6]. Although anti-PD-1 antibodies can activate anti-tumor T cells within the tumor, the limited recruitment of T cells within the tumor microenvironment (TME) means that the small number of T cells present is insufficient to exert a significant cytotoxic effect on the tumor cells [6, 7, 9]. Thus, anti-PD-1 antibodies have not achieved the desired efficacy in GBM [10]. Therefore, recruiting more tumor-specific T cells in the tumor tissue and activating their anti-tumor properties to enhance GBM patients’ response to anti-PD-1/PD-L1 antibody treatment is crucial.

Recently, researchers have explored various strategies to improve the immune microenvironment of GBM, especially the bacterial therapy, it has been demonstrated that bacteria are the most effective immune system activators [11, 12]. Bacterial therapy uses attenuated or non-toxic bacteria with unique targeting and immune activation functions, becoming a potential anti-tumor treatment [13, 14]. Facultative anaerobes or anaerobic bacteria, including *Salmonella Typhimurium*, *Clostridium novyi-NT*, *Listeria monocytogenes*, *Bifidobacterium*, and others, are capable of surviving and proliferating in the hypoxic and nutrient-rich tumor microenvironment, thereby rendering them ideal tumor-targeting vectors, can survive and proliferate in the hypoxic and

nutrient-rich tumor microenvironment, making them ideal tumor-targeting vectors [14, 15]. Among the diverse bacteria employed for tumor therapy, *Escherichia coli* (*E. coli*) stands out as a facultative anaerobe that has been demonstrated to be safe for cancer treatment and amenable to easy genetic modification [16]. Moreover, it has the ability to colonize tumors, release anti-tumor substances, and activate the host immune system, thereby inhibiting tumor cell growth [17–19]. However, despite the fact that *E. coli* can activate the tumor immune system to a certain degree, the complex immunosuppressive properties of the GBM microenvironment pose challenges, making it difficult to achieve effective treatment of GBM solely through the action of *E. coli* [7]. Therefore, *E. coli* exhibits significant potential as a reliable immune stimulant in tumor treatment, yet it needs to be used in combination with other drugs to fully exploit its synergistic effect in GBM immunotherapy.

Herein, in this study, we explored a novel therapeutic strategy using facultative anaerobic *E. coli* combined with anti-PD-1 antibody to treat GBM. After intravenous injection of *E. coli* into the GBM tumor bearing mice, we observed that *E. coli* can specifically colonize into the hypoxic region of GBM and activate the innate immune response, causing a short-term increase in innate inflammatory molecules such as tumor necrosis factor-alpha (TNF- α), interferon gamma (IFN- γ), interleukin-6 (IL-6), interleukin-1beta (IL-1 β), tumor growth factor-beta1 (TGF- β 1) and interleukin-10 (IL-10). More importantly, *E. coli* significantly activated and recruited more tumor antigen-specific CD8⁺ T cells and increased the depth of CD8⁺ T cell infiltration into the tumor tissues. In subsequent treatments, the combination of *E. coli* and anti-PD-1 antibody significantly inhibited tumor growth and extended mouse survival. We also showed that the combination therapy significantly inhibited the expression of ki67 and led to significant cell apoptosis. In summary, we propose a new strategy of bacterial therapy assisting anti-PD-1 in GBM immunotherapy, which significantly improves the efficacy of immune checkpoint blockade therapy and provides new strategy for GBM treatment.

Materials and methods

Bacteria culture

Escherichia coli (BL21) was purchased from Shanghai Weidi Biotechnology Co., Ltd (China) and stored

at -80°C . For bacterial culture, *E. coli* was cultured in Luria–Bertani (LB) liquid medium in a constant temperature oscillation incubator (37°C , 220 rpm) and these bacterial cells were harvested at the exponential growth phase. Afterward, the bacterial suspensions were washed twice and resuspended in phosphate buffer saline (PBS) buffer for the following experiments. The bacteria concentration in solution was determined by the measurement of the corresponding optical density (OD) value at 600 nm (OD_{600}), and numbers of bacterial colonies were verified by plating dilutions of inoculum onto LB agar plate.

Cell culture

The mouse glioblastoma CT2A cells were purchased commercially from the Chinese Academy of Sciences Cell Bank (China). The cells were cultured according to CBCAS recommended conditions at 37°C with 5% CO_2 in DMEM supplemented with 10% Fetal Bovine Serum (FBS) and 1% streptomycin/penicillin.

Animals model establishment and anti-PD-1 therapy

All the animal experiments and procedures were approved by Animal Ethics and Welfare Committee (AEWC) of Yan'an Hospital Affiliated to Kunming Medical University and performed under their guidelines. C57BL/6 female mouse 6–8 weeks old were purchased from Department of Experiment Animal Science, Kunming Medical University. To construct the GBM-bearing mice model, CT2A cells were suspended in PBS (2×10^6 cells in $100\ \mu\text{L}$), and the solutions were subcutaneously injected into the right flank of C57BL/6 mice. After the tumor diameter reached ~ 0.3 mm, all tumor-bearing mouse were randomly distributed into different cages for the following experiments. The anti-PD-1 antibodies used in subsequent anti-PD-1 treatments are all Anti-mouse PD-1 (CD279)-InVivo (CAS No. N/A; CLONE No. RMP1-14) produced by Selleck Technology Co., Ltd.

Biosafety of *E. coli*

Healthy C57BL/6 mouse (6–8 weeks) were used to assess the in vivo toxicity. 2×10^7 CFU live *E. coli* (selected from a series of safety experiments including different doses, data are reflected in Supplementary Information) were dissolved in a total volume of $200\ \mu\text{L}$ PBS and the solution was injected intravenously (*i.v.*). The weight of mice was monitored every day over 14 days. Blood samples were collected before (control group) and after 1, 7 and 14 days post-injection for biochemical examinations of complete blood count (white blood cell, WBC; red blood cell, RBC; platelets, PLT; hemoglobin, HGB; mean corpuscular hemoglobin, MCH; mean corpuscular volume, MCV), liver functional markers (alanine aminotransferase, ALT;

aspartate transaminase, AST), myocardial zymogram (creatine kinase, CK; L-lactate dehydrogenase, LDH-L), and kidney functional marker (blood urea nitrogen, BUN; creatinine, CREA). The major organs (heart, liver, spleen, lung, and kidney) were stained with H&E for histological analysis at the corresponding time point. In addition, to investigate its long-term safety, we conducted the same H&E staining on these organs of mice the 24th day after bacterial injection and monitored the weight changes of mouse every 2 days during this period.

Tumor-targeting ability of *E. coli*

Before and after injecting *i.v.* *E. coli* at the dose of 2×10^7 CFU ($200\ \mu\text{L}$) at the 1st, 3rd, 5th, 7th and 14th day, the main organs (heart, liver, spleen, lung, kidney, and tumor) of mice were extracted at the corresponding time points, weighed, and homogenized at 4°C in sterile PBS. Those samples were diluted (tenfold, 100-fold, etc.) and coated on LB agar plates. After 16 h of incubation, the number of *E. coli* colonies were counted. The bacterial colony count index in tissue (CFU per gram of tissue) was calculated with colony counts and tissue weights.

Cytokine quantification

We injected *E. coli* or PBS into tumor bearing mice to investigate the alteration of innate immune cytokines by *E. coli* in tumor bearing mice. Subsequently, we divided the tumor bearing mice injected with *E. coli* into four groups: control (0-h), 24-h post dose, and 48-h post dose. Tumor supernatants and serum were isolated at the corresponding time point and stored at -80°C until analysis. IL-10, TGF- β 1, IL-6, TNF α , IL-1 β , and IFN- γ from tumor supernatants and serum were quantified using Mouse IL-10 ELISA Kit (Servicebio: GEM0003-96T), Mouse TGF- β 1 ELISA Kit (GEM0051-96T), Mouse IFN- γ ELISA Kit (Servicebio: GEM0006-96T), Mouse TNF- α ELISA Kit (Servicebio: GEM0004-96T), Mouse IL-1 beta ELISA Kit (Servicebio: GEM0002-96T) and Mouse IL-6 ELISA Kit (Servicebio: GEM0001-96T). All ELISAs were run on a 96-well plate and analyzed via colorimetric readout using the Synergy Neo Microplate Reader (BioTek Instruments).

Immunofluorescence

To examine changes in the microenvironment, tumors were fixed with paraformaldehyde and embedded in paraffin. The trimmed wax block was put into a paraffin slicer for slicing, with a thickness of $4\ \mu\text{M}$. The following primary antibodies/kit are used for immunofluorescence staining: CD3 (Proteintech: 17617-1-AP, 1:500 dilution), CD4 (Proteintech: 67786-1-IG, 1:450 dilution), CD8 (Proteintech: 29896-1-AP, 1:500 dilution), FOXP3 (Proteintech: 65089-1-IG, 1:100 dilution), ki-67 (Servicebio:

GB111499, 1:500 dilution) and TMR (red) TUNEL Cell Apoptosis Detection Kit (Servicebio: G1502-50T). The secondary antibodies were used: CY3 labeled goat anti-rabbit IgG (Servicebio: GB21303, 1:300 dilution), CY3 labeled goat anti-mouse IgG (Servicebio: GB21301, 1:300 dilution), HRP tagged goat anti-rabbit IgG (Servicebio: GB23303, 1:200 dilution). Images were acquired with an upright fluorescence microscope (Nikon Eclipse C1, Nikon Japan) and scanner (Pannoramic MIDI, 3DHISTECH).

Flow cytometry

To analyze lymphocytes in tumor, spleen and blood, the tumor bearing mice was euthanized in excessive isoflurane gas chamber. Blood was obtained through enucleation method, tumor and spleen tissues were ground using frosted glass slide and fragmented tissues were incubated for 1 h at 37 °C in Collagenase/DNase solution. After passing through 70- μ m pore-sized filters to make single-cell suspension, the sample was washed three times with PBS to obtain purer single-cells suspension. Peripheral blood mononuclear cells (PBMC) were extracted from whole blood using lymphocyte separation solution. Foxp3/Transcription Factor Staining Buffer (eBioscience: 00-5523-00) was added to single-cell suspension and incubated for 30 min at room temperature and 1 mL of washing solution was added to terminate. After centrifuge at 400 r/5 min, each 5 μ L antibody solution: PerCP anti-mouse CD3 ϵ (BioLegend: 100326), FITC anti-mouse CD4 (BioLegend: 100510), APC/Fire 750 anti-mouse CD8a (BioLegend: 100766), APC anti-mouse CD25 (BioLegend: 102012) and FOXP3 Monoclonal Antibody (FJK-16 s) PE (eBioscience: 12-5773-80) were added and incubated at room temperature in the dark for 30 min. Cell precipitations after centrifugation were washed with PBS for three times, and mix well with PBS (1 mL) before testing on the flow cytometer. The results were analyzed by FlowJo software.

In vivo antitumor effect

To investigate the antitumor effect in vivo, when the tumor volumes reached approximately 20 mm³, CT2A tumor-bearing mice were randomly assigned into four groups (n=5): (1) control (saline), (2) *E. coli* only, (3) PD-1 only, (4) *E. coli*+PD-1. *Escherichia coli* solutions (2 \times 10⁷ CFU, 200 μ L) were injected *i.v.* for three consecutive days, and anti-PD-1 antibody solutions (250 μ g, 200 μ L) were injected intraperitoneally every other day for 3 consecutive times. The tumor volumes and body weights were recorded every other day during treatment. Tumor volume was calculated as $[1/2 \times \text{length} \times (\text{width})^2]$. Tumor-bearing mice were euthanized and tumor tissues were extracted to observe the tumor size when the

tumor volume approaches the ethical size of the animal. The extracted tumors were also utilized for H&E staining.

Statistical analysis

All statistical analyses were performed using SPSS 27.0 program. Data are presented as mean \pm standard deviation (SD). The significance of the differences was evaluated with Student's *t*-test and one-way ANOVA (ns: not significant, **P*<0.05, ***P*<0.01, ****P*<0.001, *****P*<0.0001).

Results

Biosafety analysis of *E. coli*

Good biosafety of *E. coli* is a prerequisite for in vivo use. We cultured *E. coli* and measured the OD values of the bacterial solution at different time points. We used the plate dilution method to obtain the growth curve of *E. coli* (Fig. 1A) and the relationship equation ($Y=37.111x-0.01645$, $R^2=0.9961$) between the OD₆₀₀ value of the bacterial solution and the number of colonies was obtained using a spectrophotometer (Figure. S1). The results showed that the logarithmic growth period of bacteria was between 2 and 4 h after bacterial culture. The maximum tolerated dose of *E. coli* is 2 \times 10¹⁰ CFU/200 μ L (Figure. S2). So, to ensure the safety of mice, we chose this dose to our following experiments. As shown in Fig. 1B, the body weight of mice showed a slight decrease trend only in the first and two post-injection days, from the 3rd post-day injection day, the body weight of mice showed an increasing trend and the trend was basically consistent with that of the control group. And after extending the time to 24 days, compared with the control group, there was no significant change in the body weight of mice injected with bacteria (Figure. S3A). This trend of weight change is basically consistent with previous studies [18, 20]. The phenomenon of weight loss in mice in the early stage may be attributed to the excessive secretion of early pro-inflammatory factors. The blood indexes including complete blood count (WBC, PLT and MCV), liver functional markers (ALT), myocardial enzymogram (LDH), and kidney functional marker (CREA) showed slight fluctuations within the safe range in early stages after *i.v.* injection, and these indicators gradually return to the normal level compared with those in the control group (post-0 day group) on the 14th day after injection (Fig. 1C). Similarly, the same trends were observed in RBC, HGB, MCH, AST, CK and BUN (Figure. S4). H&E staining showed no significant pathological damage to the major organs in each group (Fig. 1D). And after extending the time to 24 days, compared with the control group, there was no significant pathological changes were observed in important organs (Figure. S4B). These results indicated that *E. coli* with a concentration of 2 \times 10⁷ CUF

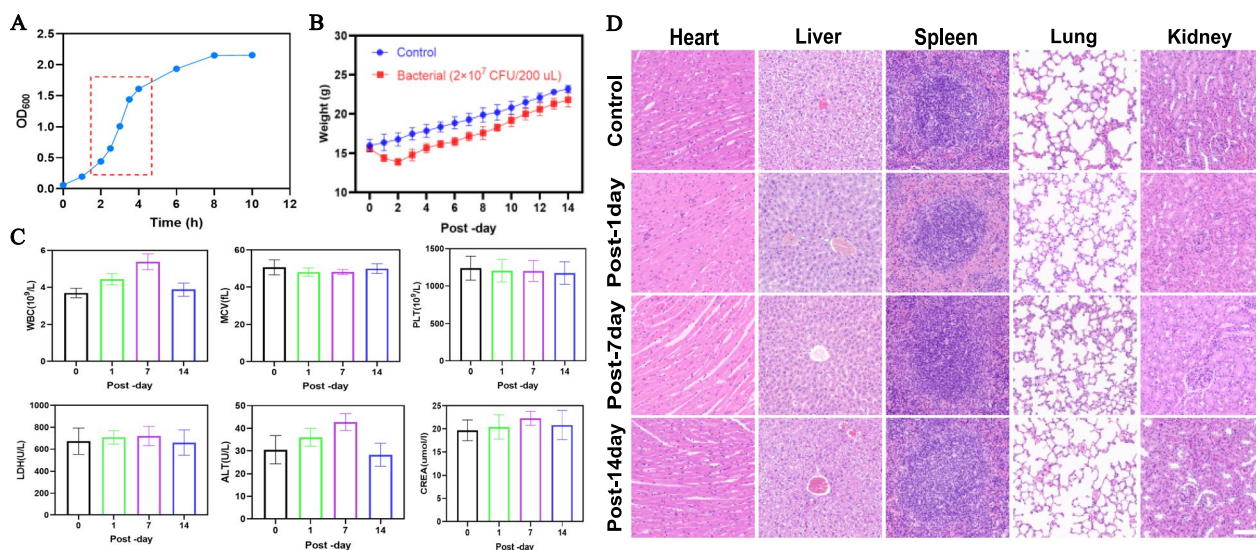


Fig. 1 Evaluation of the biosafety of *E. coli*. **A** Growth curve of *E. coli*. **B** Body weight changes of mice over various time after injection of *E. coli*. **C** Changes in organ damage serum index and complete blood count at different times. **D** H&E staining in different organs at different times after injection of *E. coli* (Scale bars: 25 μm)

(200 μL) had high biosafety in vivo, establishing their potential for further experimental application.

Distribution of *E. coli* in vivo and activated innate immune response.

To evaluate the distribution of *E. coli* in vivo, we administered the tissue homogenate on CT2A tumor bearing mice. As shown in the Fig. 2A and B, *E. coli* was gradually cleared from the organs over time and accumulated in tumor tissue, reaching about 1.28×10^7 CFU/g tissue on day 14. This phenomenon is mainly caused by the characteristics of facultative anaerobic bacteria and the immune system of the organism [19, 21]. The single colony on the plate was picked for Gram staining. Rod-shaped pink bacteria can be observed (Fig. 2C), indicating that the bacteria growth in the plate is *E. coli*. The cytokine detection results showed that type I IFN as well as a variety of proinflammatory cytokines, including IFN γ, TNF α, IL-6, and IL-1 β, were induced in a time-dependent manner in both tumor (Fig. 2D) and serum (Fig. 2E). They were highly expressed after 24 h and decreased slightly after 48 h, highlighting the activity of *E. coli* bacterial chassis [17]. Correspondingly, the decrease in expression of anti-inflammatory factors such as IL-10 at 24 h group is directly proportional to the increase in pro-inflammatory factors such as TNF-α (Fig. 2F). Based on this time-dependent characteristic, we chose to inject *E. coli* continuously for three days in subsequent experiments. Collectively, these data demonstrate the time-dependent pharmacology of *E. coli*, its tumor target engagement

in vivo and its utility as a potent inducer of local inflammation and its potential anti-tumor activity.

***Escherichia coli*-induced activation and recruitment of immune memory cells**

Next, we investigated the effect of *E. coli* on acquired immunity in tumor-bearing mice. Tumor-bearing mice treated with various agents were euthanized, tumor tissues, peripheral blood and spleen were isolated on post-10 day after *E. coli* injection. Notably, the tumor tissues, spleen and peripheral blood of the mice exhibited a significant increase in the number of immune cells in the presence of *E. coli*. Excitingly, the number of infiltrated immune cells in tumor tissue is much higher than those in peripheral blood and spleen, suggesting a role of the *E. coli* in immune cell recruitment and activation (Fig. 3A). In the tumor tissues, the abundance of CD8⁺ T cells was significantly increased compared to the control group, with the *E. coli*+PD-1, *E. coli*, and PD-1 groups being 2.08, 1.66 and 1.55 times higher respectively (Fig. 3B). Encouragingly, the activation of CD8⁺ T cells dependent on this type of *E. coli* also showed the same trend in the spleen (Fig. 3C) and peripheral blood (Fig. 3D). Furthermore, tissue immunofluorescence staining showed stronger fluorescence intensity (red represents CD8⁺ T cells) in the treatment groups compared with the control group (Fig. 3E). The relative fluorescence intensity of the *E. coli* and *E. coli*+PD-1 groups, especially *E. coli*+PD-1 group, was significantly higher than that of the other groups (Fig. 3F), which intuitively proved that *E. coli* recruited a large number of CD8⁺ T cells in the tumor.

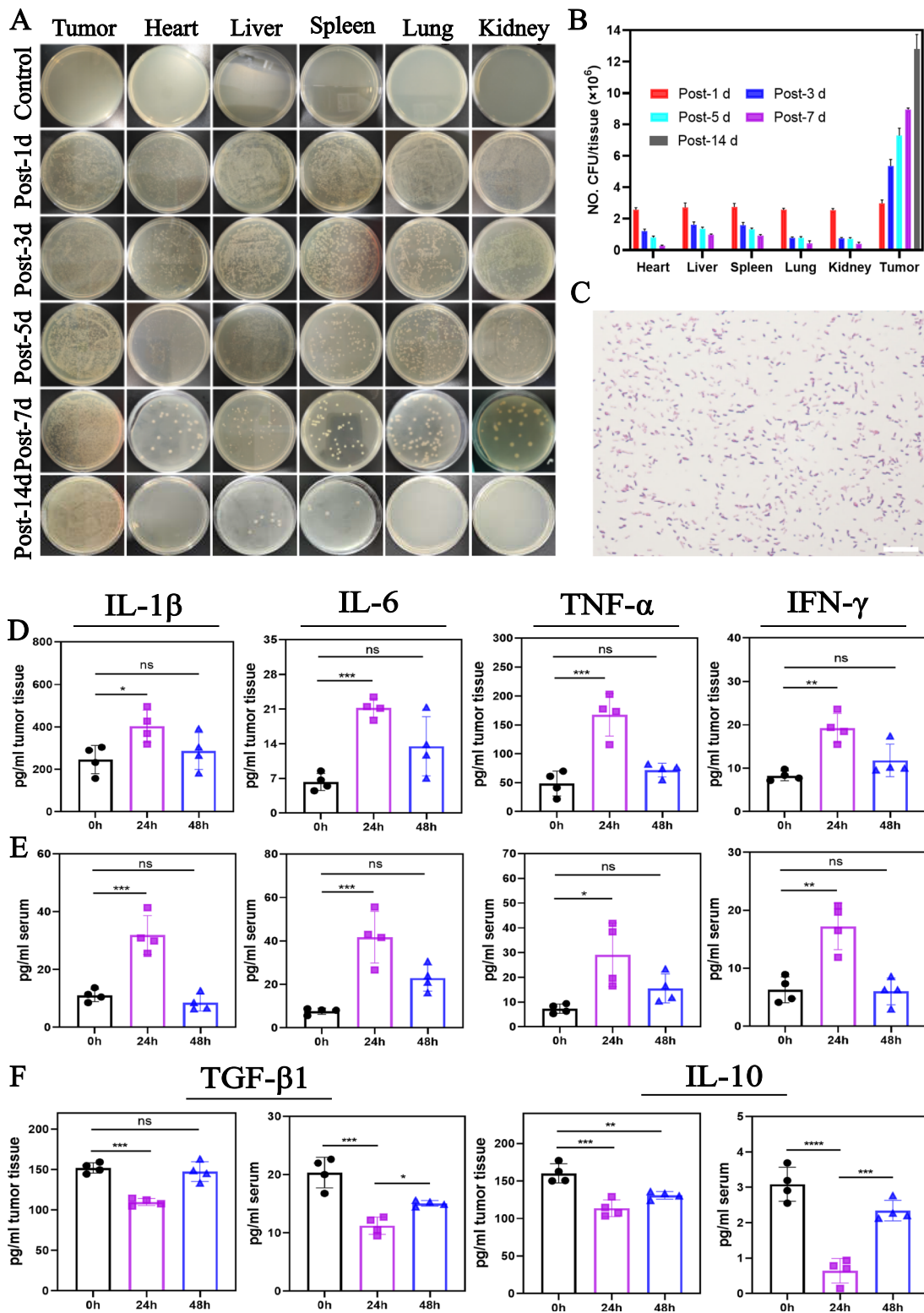


Fig. 2 Distribution of *E. coli* in tumor-bearing mice and innate immune activation. **A** Solid LB agar plates of bacterial colonization in various tissues at the indicated timepoints. **B** Quantification of bacterial colonization in various tissues. **C** Optical microscope image of gram stain of a monoclonal colony from the above LB plates (Scale bars: 25 μ m). **D, E** Cytokine abundance from tumor supernatants (**D**) and serum (**E**) for IL-1 β , IL-6, TNF α and IFN- γ from treated mice at the indicated time points after *i.v.* injection of *E. coli*. **F** Cytokine abundance from tumor tissues and serum for IL-10 and TGF- β 1, from treated mice at the indicated time points after *i.v.* injection of *E. coli* ($n=4$, ns: not significant, $*P<0.05$, $**P<0.01$, $***P<0.001$, $****P<0.0001$, calculated by one-way ANOVA)

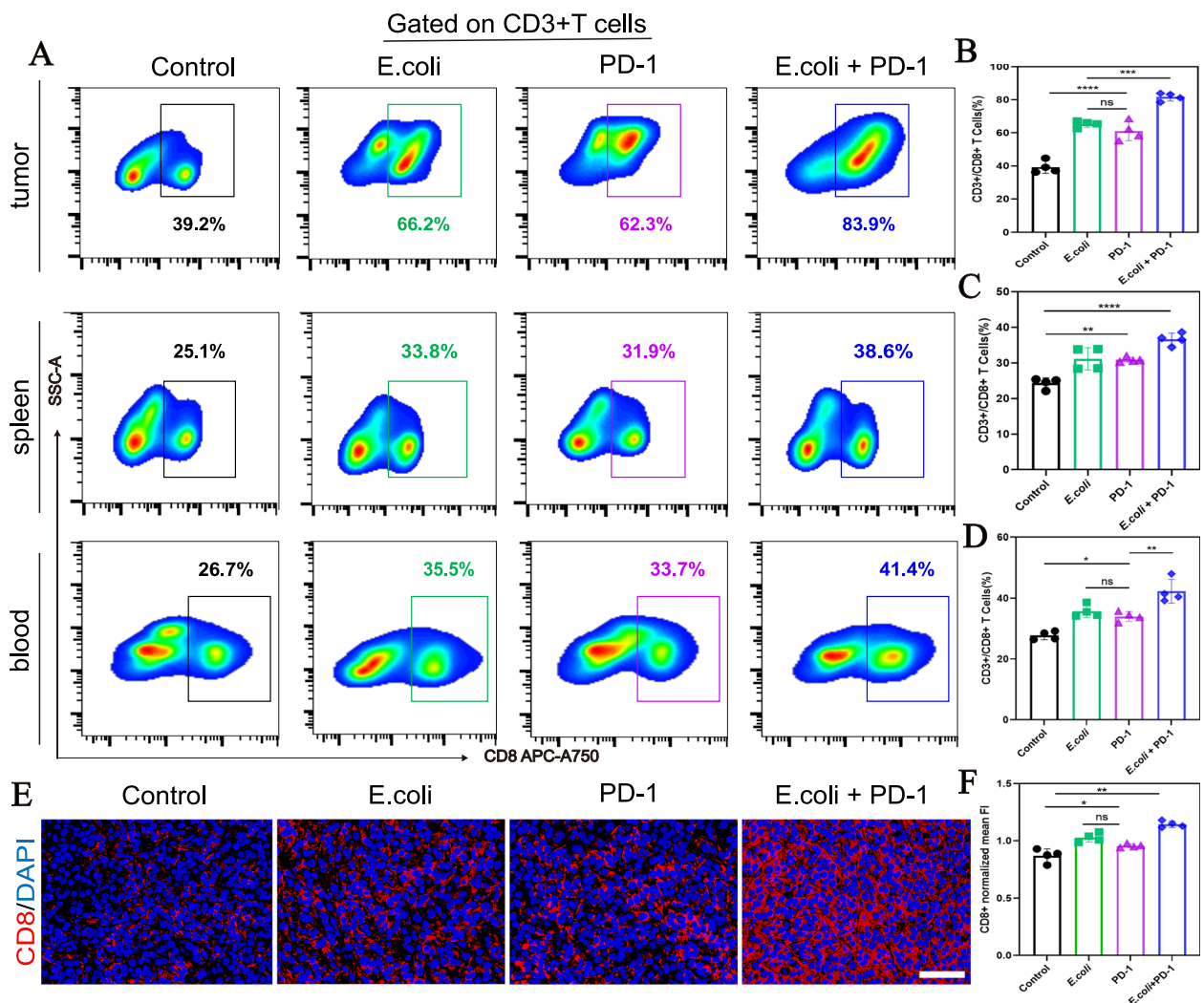


Fig. 3 Immunomodulatory efficacy of *E. coli*/PD-1 for mobilizing immunity against tumors. **A** Flow cytometry results of CD3⁺CD8⁺ T cells in tumor tissue, spleen and peripheral blood after different treatments. **B–D** Quantitative analysis of CD3⁺CD8⁺ cytotoxic T cells (n = 4). **E** Immunofluorescence staining of CD8⁺ T cells in tumor tissue (labeled with red. Scale bars: 40 μm). **F** Normalized relative fluorescence intensity (FI) (n = 4). (ns: not significant, *P < 0.05, **P < 0.01, ***P < 0.001, ****P < 0.0001, calculated by one-way ANOVA)

In addition, flow cytometry results also showed that the presence of *E. coli* promoted the infiltration of a large number of CD3⁺T cells into the tumor, which reflected the recruitment function of *E. coli* towards T cells (Figure. S5).

The synergistic treatment of *E. coli* and PD-1 reduced the infiltration of regulatory T cells

Since we have confirmed that *E. coli* can activate and recruit cytotoxic T cells within tumors, we would like to know whether *E. coli* can assist in anti-PD-1 therapy to alleviate this immunosuppression caused by the high expression of regulatory T cells in GBM tumors. Therefore, we further evaluated the regulation of regulatory

T cells by the combination therapy of *E. coli* and anti-PD-1. Flow cytometry analysis showed that both *E. coli* treatment alone and anti-PD-1 treatment alone down-regulated the infiltration level of Treg cells in the tumor compared with the PBS (control group) alone, and more remarkably, the combination therapy resulted in a further significant reduction of Treg cells (Fig. 4A, B). Moreover, it also reduced the levels of Treg cells in the spleen (Fig. 4C) and peripheral blood (Fig. 4D), although not as effectively as in the tumors (Fig. 4A). Immunofluorescence microscopy confirmed that the combination therapy further decreased Foxp3⁺ T cell (Tregs) infiltration compared to monotherapy (Fig. 4E, F). These results demonstrate that *E. coli* therapy synergistically enhances

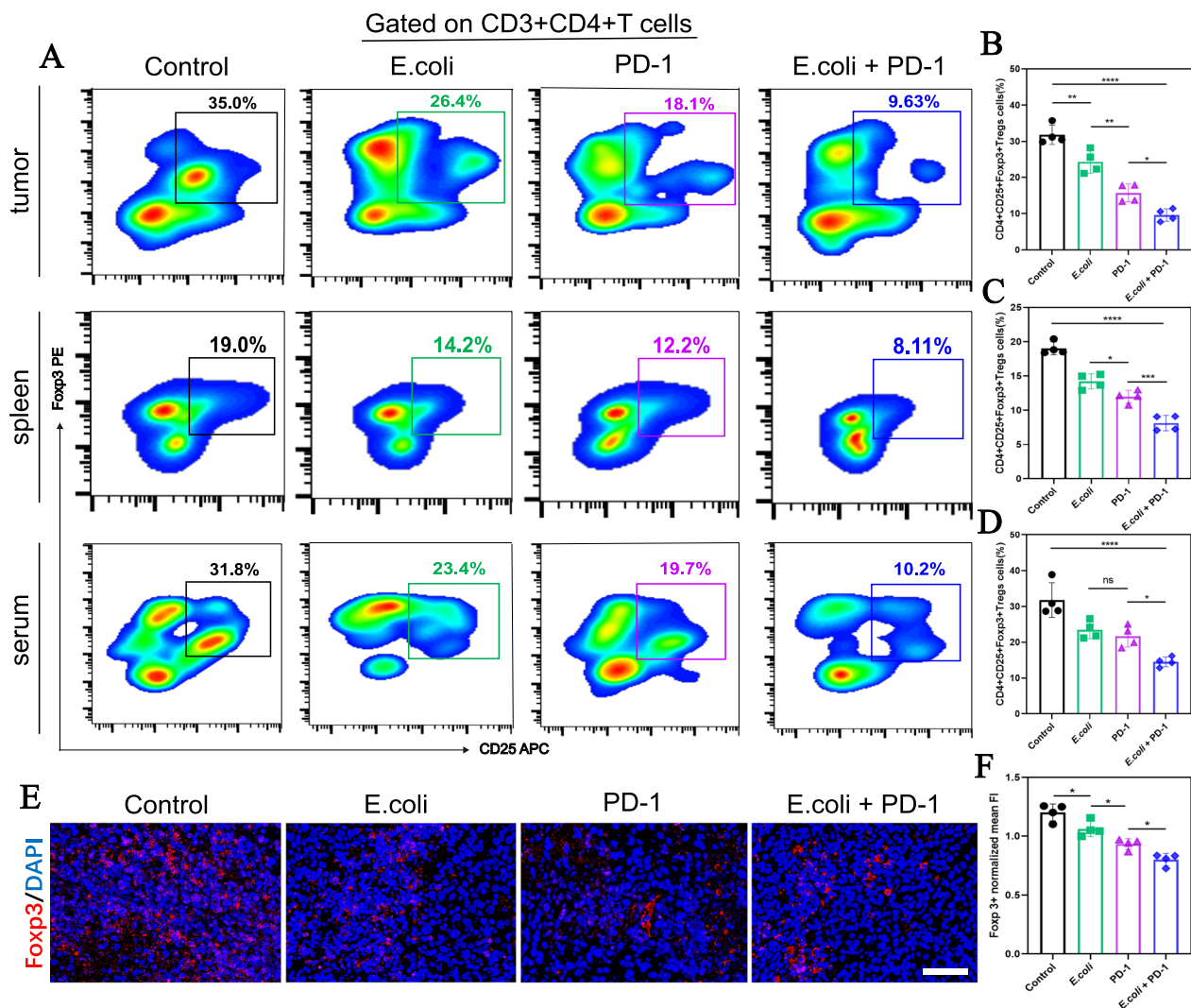


Fig. 4 Synergistic regulation of regulatory T cells by *E. coli* and PD-1. **A** Flow cytometry results of CD3⁺CD4⁺CD25⁺Foxp3⁺ T cells in tumor tissues, spleen and peripheral blood after different treatments. **B–D** Quantitative analysis of CD3⁺CD4⁺CD25⁺Foxp3⁺ regulatory T cells (n=4). **E** Immunofluorescence staining of Tregs cells in tumor (labeled with red. Scale bars: 40 μm). **F** Normalized relative fluorescence intensity. (n=4, ns: not significant, *P<0.05, **P<0.01, ***P<0.001, ****P<0.0001, calculated by one-way ANOVA)

the inhibitory effect of anti-PD-1 therapy on regulatory T cells, further demonstrating the anti-tumor potential of *E. coli*. In addition, analysis of CD8⁺Foxp3⁺T cells showed that the presence of *E. coli* reduced the number of Treg cells in CD8⁺T cells (Figure. S6), further indicating that the bacteria can recruit the CD8⁺T cells and restore the function of CD8⁺T cell.

In vivo synergistic antitumor effect

The preliminary results confirmed the effective accumulation of *E. coli* in the tumor area and its excellent ameliorative effect on the immune TME, which encouraged us to further investigate their therapeutic potential in vivo. The treatment protocol was performed according to the

treatment administration schedule (Fig. 5A). As shown in Fig. 5B and C, the tumor volume of mice treated with *E. coli* and PD-1 was smaller than the control group and the tumor volume of each group did not show statistical significance on day 0, indicating consistency in the baseline tumor volume (Figure. S7). In particular, “the *E. coli* + PD-1” treated mice showed the most significant tumor growth inhibition compared to other groups (****P<0.0001), which could be attributed to the efficient synergistic antitumor efficiency (tumor inhibition rate=63.5%) (Table. S1), stemming from the combined bacteria therapy and immunotherapy. Notably, there is no significant weight loss was observed in the tumor-bearing mice during the therapeutic period (Fig. 5D),

indicating the systemic toxicity of *E. coli* and anti-PD-1 antibody was negligible. On post-14 day of treatment, the tumor-bearing mice were euthanized and tumor tissue was extracted for weighing and photography. As shown in Fig. 5E and F. The results showed that the tumor volume of each treatment group was smaller than that of the control group, with the *E. coli*+PD-1 group being the most significant, followed by the *E. coli* group. In addition, H&E staining, TUNEL and Ki67 immunofluorescence staining (Fig. 5G) further confirmed that *E. coli* enhanced anti-PD-1 immunotherapy effect. H&E staining showed clearly abnormal nuclei (karyopyknosis, karyorrhexis, and karyolysis) of tumor cells in each treatment group compared with the control group, with the *E. coli*+PD-1 group being the most significant. Similarly, the mice treatment with “the *E. coli*+PD-1” displayed negligible proliferation (Ki67, red) and significant apoptosis (TUNEL, red) compared to the control group. The quantified fluorescence results also showed the inhibition of tumor proliferation and promotion of apoptosis by combination therapy (Figure. S8).

Discussion

GBM represents a major therapeutic challenge due to its aggressive nature and the limited efficacy of current ICB therapies. Our study aimed to address this challenge by combining *E. coli* with anti-PD-1 antibodies to enhance the immune response against GBM. This approach capitalizes on the ability of bacteria to induce immune activation within tumors, a strategy previously explored with varying success in different cancer types [17, 21]. Our findings underscore the potential of *E. coli* to activate the innate immune system within GBM and to enhance the efficacy of anti-PD-1 therapy, as evidenced by the increased cytotoxic CD8⁺ T cells and decreased regulatory T-cells. In addition, decreased Ki67 and increased TUNEL further demonstrate the inhibitory effect of this treatment on tumor cells. In conclusion, our results fully support the potential of *E. coli* as an adjuvant for glioma immunotherapy.

The role of *E. coli* in immune activation has been explored in various contexts, with studies suggesting that bacteria can stimulate the immune system by presenting tumor-associated antigens and promoting immune

cell activation [14]. In our study, *E. coli* was observed to accumulate in tumor tissues, which is consistent with previous research findings, demonstrating bacteria can specially target the tumor and colonize in the tumor tissues [18]. It has been reported that bacteria contain several pathogen-related molecular patterns, such as peptidoglycan, lipopolysaccharide (LPS), chemokines and flagellin, all of which have the ability to activate innate immune signaling pathways, and induce the secretion of significant amounts of cytokines and chemokines [22–24]. In contrast to the elevation of these pro-inflammatory factors, we observed a decrease in anti-inflammatory factors, which may be attributed to bacterial induced macrophage polarization. Research has shown that bacteria can induce polarization of macrophages, which can increase the secretion of TNF- α and IL-6, and inhibit the secretion of IL-10 and TGF- β [25]. Our study observed that the activation of innate immunity in mice by *E. coli* can only last for one day, which is similar to the Huang’ results [26]. This is also the reason why we chose to inject *E. coli* continuously. Furthermore, inflammatory response induced by bacterial lysates are also involved in the activation of adaptive immune cells, making the TME more conducive to T cell infiltration [27]. This shift from an immune-cold to an immune-hot environment enhances the overall efficacy of immunotherapy. These completed studies suggest that the strategy of activating innate and adaptive immunity via bacteriotherapy is a practical way to reverse the immunosuppressive microenvironment and promote the formation of anti-tumor immune memory [27–29]. In our study, the high expression of innate immune factors such as TNF- α and IL-1 β is more significant in tumor tissues than serum. The reason for this result may be due to *E. coli*’s intrinsic tumor tropism, this immunostimulatory results in a cytokine response concentrated to the TME [17]. This is advantageous from a safety perspective and this chemokine gradients are conducive to steer immune cell trafficking into the tumor [17, 30]. In our murine tumor models, *E. coli* treatment resulted in the establishment of immunological memory, such as the increased infiltration of acquired immune cells such as CD8⁺ T cells, are highly consistent with this conclusion, demonstrating the effectiveness of *E. coli* in anti-tumor immunotherapy.

(See figure on next page.)

Fig. 5 The synergistic anti-tumor effect of combination therapy. **A** The treatment protocol. **B** Tumor growth trajectories of CT2A tumor-bearing mice following various treatments (n=5, ns: not significant, * $P < 0.05$, ** $P < 0.01$, *** $P < 0.001$, **** $P < 0.0001$, calculated by one-way ANOVA). **C** Digital photos of CT2A tumor-bearing mice during the therapeutic period. **D** Body weight curves of CT2A tumor-bearing mice across different treatment groups (n=5, values are means \pm SD). **E** Quantification of tumor weights at 14 days post various treatments (n=5, values are means \pm SD, ns: not significant, * $P < 0.05$, ** $P < 0.01$, *** $P < 0.001$, **** $P < 0.0001$, calculated by one-way ANOVA). **F** Digital photos of the excised tumors collected after 14 days. **G** H&E (Scale bars: 40 μ m), TUNEL (Scale bars: 40 μ m) and Ki67 (Scale bars: 40 μ m) staining of the tumor tissue after various treatments

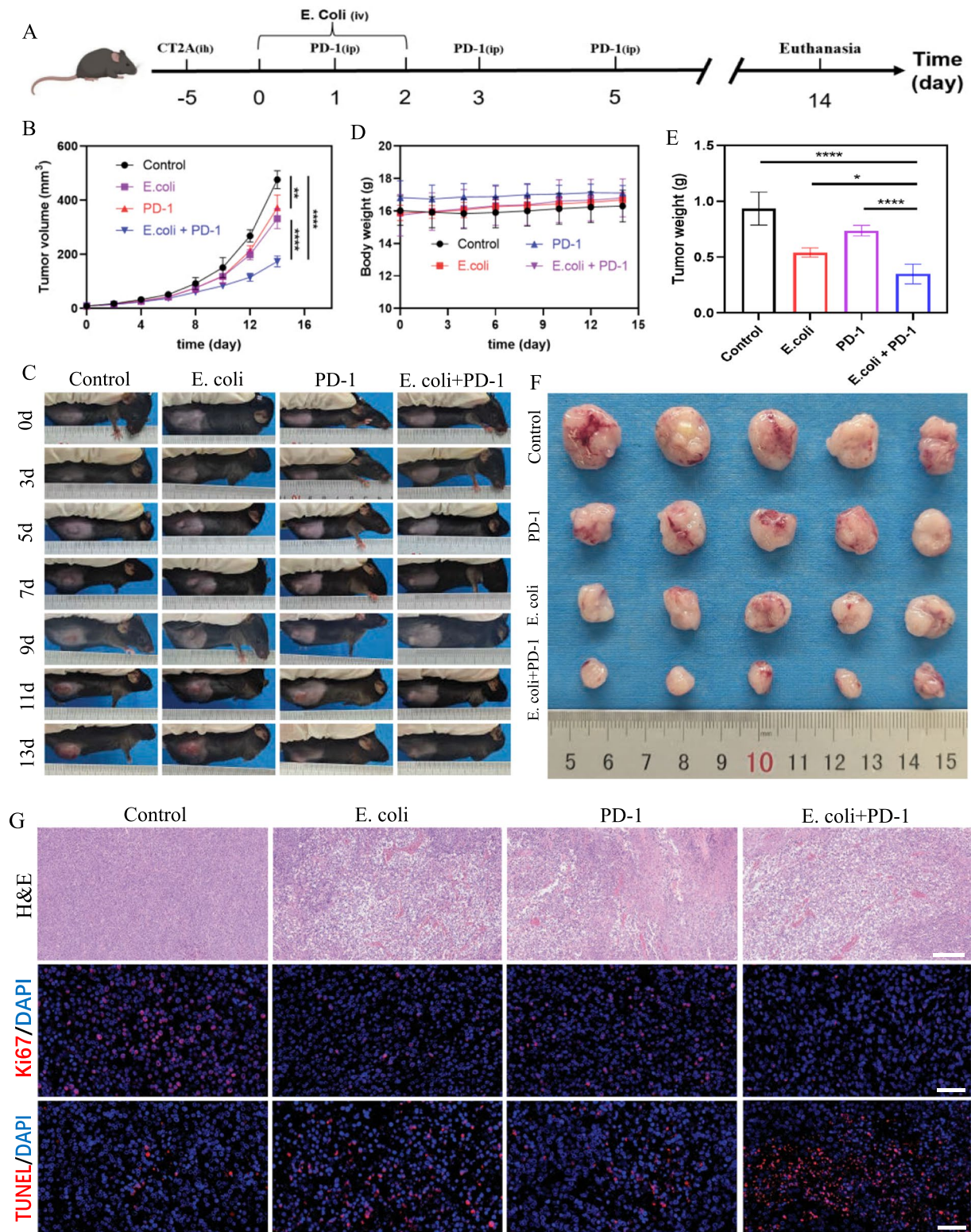


Fig. 5 (See legend on previous page.)

Interestingly, our study revealed a significant increase in T cell infiltration within the tumor compared to relatively lower levels observed in the peripheral blood and spleen. This phenomenon can be attributed to the unique alterations in TME induced by the presence of *E. coli* [31, 32]. The colonization of hypoxic regions by these bacteria likely creates a localized inflammatory milieu, that is conducive to attracting T cells from the peripheral circulation [33]. Once these T cells migrate into the TME, they may become sequestered due to the presence of various chemokines and cytokines that promote their retention within the tumor [27]. This retention process is critical, as it results in a localized concentration of T cells precisely where they are most needed for effective antitumor responses. Consequently, this could explain the lower T cell counts observed in the blood and spleen compared to the tumor tissue. The retention of T cells within the tumor site is a crucial aspect of effective immunotherapy [34]. By ensuring that immune effector cells are concentrated at the tumor location, the treatment can effectively focus the immune response on eliminating tumor cells [35]. This mechanism may contribute to the enhanced antitumor efficacy observed with the combination of *E. coli* and anti-PD-1.

The synergistic mechanism of *E. coli* and anti-PD-1 therapy reveals a complex interaction between bacterial-induced immune activation and checkpoint inhibition. While previous research has explored the individual effects of bacterial therapies and immune checkpoint inhibitors [7, 36], our study provides a unique perspective on their combined effect in GBM. T cell exhaustion caused by the interactions between PD-1 and PD-L1/2 is one of the key features of cancer [37]. PD-1/PD-L1 targeted immunotherapy have been widely used to reinvigorate these exhausted T cells for anti-cancer therapy. Thus, overcoming the immunosuppressive environment of solid tumor by recruiting cancer-specific T cells is critical to improve therapeutic efficacy of PD-1/PD-L1 therapy [38]. The enhanced immune activation observed in our study suggests that tumor colonization of *E. coli* caused not only effective infiltration of the activated cancer-specific CD8⁺ T cells into the TME, but also down-regulation of the expression level of regulatory T cell markers. These phenomena indicate that *E. coli* may not only prime the immune system but also create a more favorable environment for anti-PD-1 therapy. In fact, the blockade of PD-1 and PD-L1 binding by anti-PD-1 antibodies can only restore the activity of T cells, enabling them to recognize and kill tumor cells, but cannot change the immune-cold TME [39, 40]. And the role of bacteria is precisely to recruit more T cells for tumors [41]. Therefore, we combined the two, with bacteria are responsible for recruiting T cells, and anti-PD-1 antibodies

responsible for restoring the tumor-killing function of T cells, to achieve effective anti-tumor effects. And the combination of *E. coli* or its derivatives with anti-PD-1 therapy has achieved preliminary results in the study of melanoma [42]. This complementary combination approach could be a valuable addition to the GBM treatment armamentarium.

Despite the promising findings of this study, several limitations must be acknowledged. First, the use of a subcutaneous mouse model, while providing important insights, may not fully capture the complexity of the human tumor microenvironment, particularly in the context of GBM [2]. The immune system and tumor-immune interactions in humans are more complex, and the efficacy observed in murine models may not directly translate to clinical settings [43]. Secondly, the mechanism of tumor immune evasion is complex. GBM is a highly heterogeneous and aggressive malignancy with complex immune evasion mechanisms [44]. While this study partially elucidates the modulation of the immune microenvironment by the combined therapy, it may not fully explore all possible immune evasion pathways. Additionally, while *E. coli* demonstrated tumor-targeting capabilities and contributed to immune activation, its long-term biosafety, particularly concerning potential off-target effects or systemic infections, requires further investigation in more comprehensive preclinical and clinical studies [11].

Moving forward, this research opens new avenues for combining bacterial-based therapies with immune checkpoint inhibitors like anti-PD-1. Exploring the mechanisms underlying the interaction between bacteria and immune cells could lead to the development of more targeted bacterial therapies. Moreover, it is worth exploring the use of biotechnology to modify *E. coli* to carry anti-tumor genes/substances. The integration of bacterial-based immunotherapy into the broader landscape of GBM treatment, including its combination with radiotherapy or chemotherapy, is another potential direction for enhancing patient outcomes.

Conclusions

In conclusion, this study provides compelling evidence for the use of *E. coli* as an adjuvant to enhance the efficacy of anti-PD-1 immunotherapy in GBM. By modulating the TME to increase immune cell infiltration and reducing Treg levels, *E. coli* significantly improves the antitumor response in this challenging malignancy. The observed discrepancy in T cell levels between the tumor and peripheral sites highlights the importance of localizing the immune response to the tumor, a key factor in the success of this therapeutic strategy.

Abbreviations

ALT	Alanine transaminase
AST	Aspartate transaminase
BUN	Blood urea nitrogen
CFU	Colony-forming units
CK	Creatine kinase
CREA	Creatinine
<i>E. coli</i>	<i>Escherichia coli</i>
FBS	Fetal bovine serum
PBMC	Peripheral blood mononuclear cells
H&E	Hematoxylin and Eosin
HGB	Hemoglobin
LB	Luria–Bertani
LDH	Lactate dehydrogenase
LPS	Lipopolysaccharide
MCH	Mean corpuscular hemoglobin
MCV	Mean corpuscular volume
OD	Optical density
PBS	Phosphate buffer saline
PLT	Platelets
RBC	Red blood cell
TUNEL	TdT-mediated dUTP Nick-End labeling
WBC	White blood cell
GBM	Glioblastoma multiforme
ICB	Immune checkpoint blockade
ELISA	Enzyme linked immunosorbent assay
BBB	Blood–brain barrier
PD-1	Programmed cell death protein-1
PD-L1	Programmed cell death-ligand 1
NSCLC	Non-small cell lung cancer
IL-6	Interleukin-6
TNF α	Tumor necrosis factor- α
IL-1 β	Interleukin-1beta
IFN- γ	Interferon-gamma
FI	Fluorescence intensity
IRT	Tumor inhibition rate

Supplementary Information

The online version contains supplementary material available at <https://doi.org/10.1186/s12967-025-06194-y>.

Supplementary Material 1.

Acknowledgements

Thanks for all participants involved in this research.

Author contributions

Guochen Li, Haiyan Yang and Guangrong Zheng conceived the design and carried out the experiments, and wrote the manuscript. Xiaolan Du, Xirui Duan and Tengfei Ke analyzed the data. Xinyan Zhou and Na Tan revised the manuscript and prepared the figures. Chengde Liao provides most of financial support for all experiments. All authors read and approved the final manuscript.

Funding

This work was supported by National Natural Science Foundation of China (Grant No. 82160340), Yunnan Talents Support Program (Grant No. XDYC-MY-2022-0064), Natural Science Foundation of Chongqing (Grant No. CSTB2024NSCQ-MSX0102), Chongqing Postdoctoral Science Foundation (Grant No. 2023CQBSHTB1005), Chongqing Medical Youth Top-notch Talent (Grant No. YXQN 202446) and Graduate Innovation Foundation of Kunming Medical University (Grant No. 2024S122, 2024B013).

Availability of data and materials

The data sets used and/or analyzed during the current study are available from the corresponding author on reasonable request.

Declarations

Ethics approval and consent to participate

The animal procedures were authorized by the Animal Ethics and Welfare Committee (AEWC) of Yan'an Hospital Affiliated to Kunming Medical University (Approval NO. 20231115).

Consent for publication

Not applicable.

Competing interests

The authors declare that they have no competing interests.

Author details

¹Department of Radiology, Yan'an Hospital of Kunming City (Yan'an Hospital Affiliated to Kunming Medical University, Yunnan Cardiovascular Hospital), Kunming, China. ²Department of Ultrasound, Chongqing General Hospital, Chongqing University, Chongqing, China. ³Department of Radiology, Yunnan Cancer Hospital (The Third Affiliated Hospital of Kunming Medical University, Peking University Cancer Hospital Yunnan Campus), Kunming, China.

Received: 17 October 2024 Accepted: 30 January 2025

Published online: 07 February 2025

References

- Sabu A, Liu T-I, Ng SS, Doong R-A, Huang Y-F, Chiu H-C. Nano-medicines targeting glioma stem cells. *ACS Appl Mater Interfaces*. 2023;15(1):158–81.
- Jayaram MA, Phillips JJ. Role of the microenvironment in glioma pathogenesis. *Annu Rev Pathol*. 2024;19:181–201.
- Kumari S, Gupta R, Ambasta RK, Kumar P. Multiple therapeutic approaches of glioblastoma multiforme: from terminal to therapy. *Biochim Biophys Acta Rev Cancer*. 2023;1878(4):188913.
- Song X, Qian H, Yu Y. Nanoparticles mediated the diagnosis and therapy of glioblastoma: bypass or cross the blood-brain barrier. *Small*. 2023;19(45): e2302613.
- Yasinjan F, Xing Y, Geng H, Guo R, Yang L, Liu Z, Wang H. Immunotherapy: a promising approach for glioma treatment. *Front Immunol*. 2023;14:1255611.
- Pombo Antunes AR, Scheyltjens I, Duerinckx J, Neyns B, Movahedi K, Van Ginderachter JA. Understanding the glioblastoma immune microenvironment as basis for the development of new immunotherapeutic strategies. *Elife*. 2020;9: e52176.
- Rahman M, Sawyer WG, Lindhorst S, Deleyrolle LP, Harrison JK, Karachi A, Dastmalchi F, Flores-Toro J, Mitchell DA, Lim M, et al. Adult immunoncology: using past failures to inform the future. *Neuro Oncol*. 2020;22(9):1249–61.
- Sordo-Bahamonde C, Lorenzo-Herrero S, Granda-Díaz R, Martínez-Pérez A, Aguilar-García C, Rodrigo JP, García-Pedrero JM, Gonzalez S. Beyond the anti-PD-1/PD-L1 era: promising role of the BTLA/HVEM axis as a future target for cancer immunotherapy. *Mol Cancer*. 2023;22(1):142.
- Liu H, Zhao Q, Tan L, Wu X, Huang R, Zuo Y, Chen L, Yang J, Zhang Z-X, Ruan W, et al. Neutralizing IL-8 potentiates immune checkpoint blockade efficacy for glioma. *Cancer Cell*. 2023;41(4):693.
- Ott M, Tomaszowski K-H, Marisetty A, Kong L-Y, Wei J, Duna M, Blumberg K, Ji X, Jacobs C, Fuller GN, et al. Profiling of patients with glioma reveals the dominant immunosuppressive axis is refractory to immune function restoration. *JCI Insight*. 2020;5(17): e134386.
- Gurbatri CR, Arpaia N, Danino T. Engineering bacteria as interactive cancer therapies. *Science*. 2022;378(6622):858–64.
- Shen X, Zhu C, Liu X, Zheng H, Wu Q, Xie J, Huang H, Liao Z, Shi J, Nan K, et al. Engineered bacteria for augmented in situ tumor vaccination. *Biomater Sci*. 2023;11(4):1137–52.
- Pulendran B, Arunachalam PS, O'Hagan DT. Emerging concepts in the science of vaccine adjuvants. *Nat Rev Drug Discov*. 2021;20(6):454–75.
- Tang Q, Peng X, Xu B, Zhou X, Chen J, Cheng L. Current status and future directions of bacteria-based immunotherapy. *Front Immunol*. 2022;13:911783.

15. Shi H, Chen L, Liu Y, Wen Q, Lin S, Wen Q, Lu Y, Dai J, Li J, Xiao S, et al. Bacteria-driven tumor microenvironment-sensitive nanoparticles targeting hypoxic regions enhances the chemotherapy outcome of lung cancer. *Int J Nanomed*. 2023;18:1299–315.
16. Luke JJ, Piha-Paul SA, Medina T, Verschraegen CF, Varterasian M, Brennan AM, Riese RJ, Sokolovska A, Strauss J, Hava DL, et al. Phase I study of SYN1891, an engineered *E. coli* nissle strain expressing STING agonist, with and without atezolizumab in advanced malignancies. *Clin Cancer Res*. 2023;29(13):2435–44.
17. Leventhal DS, Sokolovska A, Li N, Plescia C, Kolodziej SA, Gallant CW, Christmas R, Gao J-R, James MJ, Abin-Fuentes A, et al. Immunotherapy with engineered bacteria by targeting the STING pathway for anti-tumor immunity. *Nat Commun*. 2020;11(1):2739.
18. Sun R, Liu M, Lu J, Chu B, Yang Y, Song B, Wang H, He Y. Bacteria loaded with glucose polymer and photosensitive ICG silicon-nanoparticles for glioblastoma photothermal immunotherapy. *Nat Commun*. 2022;13(1):5127.
19. Yang H, Jiang F, Ji X, Wang L, Wang Y, Zhang L, Tang Y, Wang D, Luo Y, Li N, et al. Genetically engineered bacterial protein nanoparticles for targeted cancer therapy. *Int J Nanomed*. 2021;16:105–17.
20. Lu J, Ding J, Chu B, Ji C, Zhang Q, Xu Y, Song B, Wang H, He Y. Inactive Trojan bacteria as safe drug delivery vehicles crossing the blood-brain barrier. *Nano Lett*. 2023;23(10):4326–33.
21. Qin W, Xu W, Wang L, Ren D, Cheng Y, Song W, Jiang T, Ma L, Zhang C. Bacteria-elicited specific thrombosis utilizing acid-induced cytolysin A expression to enable potent tumor therapy. *Adv Sci*. 2022;9(15):e2105086.
22. Chen X, Li P, Luo B, Song C, Wu M, Yao Y, Wang D, Li X, Hu B, He S, et al. Surface mineralization of engineered bacterial outer membrane vesicles to enhance tumor photothermal/immunotherapy. *ACS Nano*. 2024;18(2):1357–70.
23. Duong MT-Q, Qin Y, You S-H, Min J-J. Bacteria-cancer interactions: bacteria-based cancer therapy. *Exp Mol Med*. 2019;51(12):1–15.
24. Lou X, Chen Z, He Z, Sun M, Sun J. Bacteria-mediated synergistic cancer therapy: small microbiome has a big hope. *Nanomicro Lett*. 2021;13(1):37.
25. Wei B, Pan J, Yuan R, Shao B, Wang Y, Guo X, Zhou S. Polarization of tumor-associated macrophages by nanoparticle-loaded escherichia coli combined with immunogenic cell death for cancer immunotherapy. *Nano Lett*. 2021;21(10):4231–40.
26. Huang L, Tang W, He L, Li M, Lin X, Hu A, Huang X, Wu Z, Wu Z, Chen S, et al. Engineered probiotic *Escherichia coli* elicits immediate and long-term protection against influenza A virus in mice. *Nat Commun*. 2024;15(1):6802.
27. Zhang Y, Xi K, Fu Z, Zhang Y, Cheng B, Feng F, Dong Y, Fang Z, Zhang Y, Shen J, et al. Stimulation of tumoricidal immunity via bacteriotherapy inhibits glioblastoma relapse. *Nat Commun*. 2024;15(1):4241.
28. Liu G, Ma N, Cheng K, Feng Q, Ma X, Yue Y, Li Y, Zhang T, Gao X, Liang J, et al. Bacteria-derived nanovesicles enhance tumour vaccination by trained immunity. *Nat Nanotechnol*. 2024;19(3):387–98.
29. Wang C, Zhong L, Xu J, Zhuang Q, Gong F, Chen X, Tao H, Hu C, Huang F, Yang N, et al. Oncolytic mineralized bacteria as potent locally administered immunotherapeutics. *Nat Biomed Eng*. 2024;8(5):561–78.
30. Mempel TR, Lill JK, Altenburger LM. How chemokines organize the tumour microenvironment. *Nat Rev Cancer*. 2024;24(1):28–50.
31. Chowdhury S, Castro S, Coker C, Hinchliffe TE, Arpaia N, Danino T. Programmable bacteria induce durable tumor regression and systemic antitumor immunity. *Nat Med*. 2019;25(7):1057–63.
32. Mughal MJ, Kwok HF. Multidimensional role of bacteria in cancer: mechanisms insight, diagnostic, preventive and therapeutic potential. *Semin Cancer Biol*. 2022;86(Pt 2):1026–44.
33. Zitvogel L, Ayyoub M, Routy B, Kroemer G. Microbiome and anticancer immunosurveillance. *Cell*. 2016;165(2):276–87.
34. Tsimberidou A-M, Van Morris K, Vo HH, Eck S, Lin Y-F, Rivas JM, Andersson BS. T-cell receptor-based therapy: an innovative therapeutic approach for solid tumors. *J Hematol Oncol*. 2021;14(1):102.
35. Liu X, Hoft DF, Peng G. Tumor microenvironment metabolites directing T cell differentiation and function. *Trends Immunol*. 2022;43(2):132–47.
36. Ghosh MK, Kumar S, Begam S, Ghosh S, Basu M. GBM immunotherapy: exploring molecular and clinical frontiers. *Life Sci*. 2024;356:123018.
37. McLane LM, Abdel-Hakeem MS, Wherry EJ. CD8 T cell exhaustion during chronic viral infection and cancer. *Annu Rev Immunol*. 2019;37:457–95.
38. Yi M, Zheng X, Niu M, Zhu S, Ge H, Wu K. Combination strategies with PD-1/PD-L1 blockade: current advances and future directions. *Mol Cancer*. 2022;21(1):28.
39. Bonaventura P, Shekarian T, Alcazer V, Valladeau-Guilemond J, Valsesia-Wittmann S, Amigorena S, Caux C, Depil S. Cold tumors: a therapeutic challenge for immunotherapy. *Front Immunol*. 2019;10:168.
40. Iwai Y, Hamanishi J, Chamoto K, Honjo T. Cancer immunotherapies targeting the PD-1 signaling pathway. *J Biomed Sci*. 2017;24(1):26.
41. Savage TM, Vincent RL, Rae SS, Huang LH, Ahn A, Pu K, Li F, de Los Santos-Alexis K, Coker C, Danino T, et al. Chemokines expressed by engineered bacteria recruit and orchestrate antitumor immunity. *Sci Adv*. 2023;9(10):eadc9436.
42. Jeong Y, Kim GB, Ji Y, Kwak G-J, Nam G-H, Hong Y, Kim S, An J, Kim SH, Yang Y, et al. Dendritic cell activation by an *E. coli*-derived monophosphoryl lipid A enhances the efficacy of PD-1 blockade. *Cancer Lett*. 2020;472:19–28.
43. Hicks WH, Bird CE, Pernik MN, Haider AS, Dobariya A, Abdullah KG, Aoun SG, Bentley RT, Cohen-Gadol AA, Bachoo RM, et al. Large animal models of glioma: current status and future prospects. *Anticancer Res*. 2021;41(11):5343–53.
44. Vinay DS, Ryan EP, Pawelec G, Talib WH, Stagg J, Elkord E, Lichtor T, Decker WK, Whelan RL, Kumara HMCS, et al. Immune evasion in cancer: mechanistic basis and therapeutic strategies. *Semin Cancer Biol*. 2015;35(Suppl):S185–98.

Publisher's Note

Springer Nature remains neutral with regard to jurisdictional claims in published maps and institutional affiliations.